IOP Conf. Series: Materials Science and Engineering **278** (2017) 012054 doi:10.1088/1757-899X/278/1/012054

Thermal interface material characterization for cryogenic electronic packaging solutions

A Dillon, K McCusker, J Van Dyke, B Isler and M Christiansen

Northrop Grumman Corporation, Mission Systems Sector, 1580-A West Nursery Road, Linthicum Maryland 21090, USA

Alison.Dillon@ngc.com

Abstract. As applications of superconducting logic technologies continue to grow, the need for efficient and reliable cryogenic packaging becomes crucial to development and testing. A trade study of materials was done to develop a practical understanding of the properties of interface materials around 4 K. While literature exists for varying interface tests, discrepancies are found in the reported performance of different materials and in the ranges of applied force in which they are optimal. In considering applications extending from top cooling a silicon chip to clamping a heat sink, a range of forces from approximately 44 N to approximately 445 N was chosen for testing different interface materials. For each range of forces a single material was identified to optimize the thermal conductance of the joint. Of the tested interfaces, indium foil clamped at approximately 445 N showed the highest thermal conductance. Results are presented from these characterizations and useful methodologies for efficient testing are defined.

1. Introduction

Predicting the contact conductance across an interface has historically been one of the most difficult aspects of cryogenic design. With thermal performance being a function of bulk material, interface material, clamping force, surface roughness and surface oxides, the sheer number of variables in any given experiment requires a large test matrix to understand the impact of each. When looking to design packaging for superconducting electronics operating very close to liquid helium temperatures (4.2 K), the need for a high level of confidence in the performance of the designs is critical to success. A review of literature available for contact conductance characterization yielded a large sum of somewhat contradicting data points. The contradiction comes from the inevitable variability of many of the parameters mentioned above. An effort must be made during experiment design to match the predicted conditions of the desired packaging interfaces as closely as possible in order to reduce the error that results from data extrapolation.

The goal of this effort was to continue to identify interface materials that had the best thermal performance for given bulk materials in different force ranges. The scope of this paper covers a sub-set of the total planned experiments in this study, focusing on the basic copper-copper interfaces that were tested to allow result comparison with literature and to identify any key differences in the predicted performance. In this paper the temperature gradient of interest, ΔT_{TIM}, was calculated using equation (1) and the thermal conductance across each interface, G, was calculated using equation (2). Equation (3) was used to calculate the amount of measured temperature difference that occurred in the copper sample and interposer rather than across the thermal interface material.

$$\Delta T_{TIM} = T_S - T_{Int} - \Delta T_{Cu} \quad (1)$$

$$G = \frac{Q}{\Delta T_{TIM}} \quad (2)$$

$$\Delta T_{Cu} = Q\left(\frac{L}{k_{Cu}A}\right) \quad (3)$$

In the equations above, T represents temperature with the subscripts TIM, S, Int, and Cu representing the thermal interface material, the copper sample, the copper interposer, and copper, respectively. The applied power is represented by Q, the thermal conductivity by k, the contact surface area by A, and the material length between the thermal interface and the temperature sensor bobbins by L.

2. Test Setup

The unit under test consisted of an Oxygen-Free High thermal Conductivity (OFHC) copper sample which was attached to an OFHC copper interposer using the thermal interface material to be tested. This assembly also contained two commercially calibrated Cernox CX-1050-CU-HT temperature sensor bobbins to monitor the temperature rise through the thermal interface material and one Kapton heater to drive that temperature delta. A low or medium force head assembly was attached to the interposer providing a consistent clamping force. Stainless steel was selected for all pieces outside the critical heat path in order to minimize heat leak. The full assembly is shown in Figure 1.

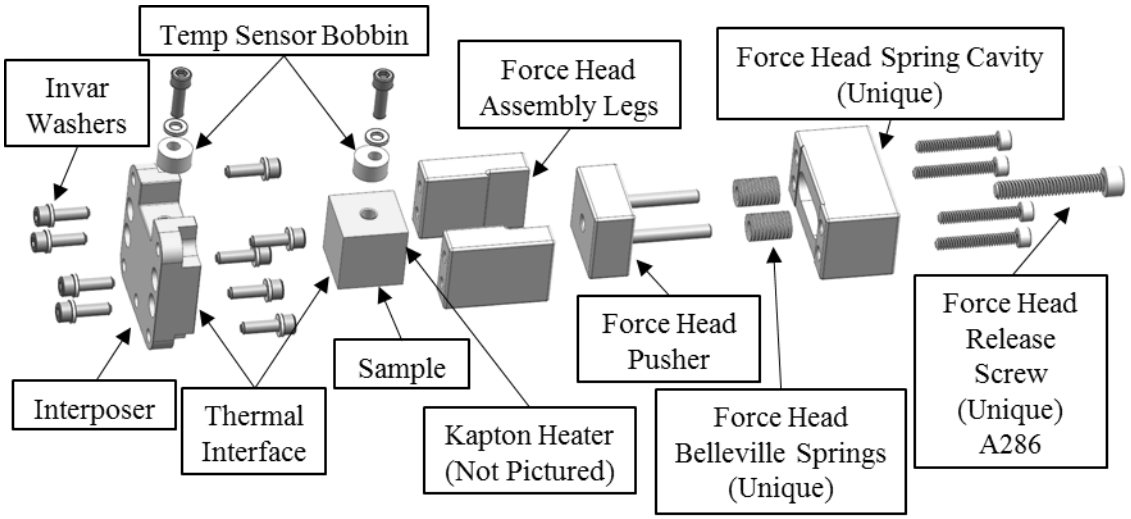

Figure 1. Full test assembly.

Two temperature sensor bobbins were secured to the interposer and the copper sample using a 2.845 mm (#4) socket head screw and a 3.175 mm ID (#4) washer. A Kapton heater was mounted to the top of the copper sample using pressure sensitive adhesive. The specific temperature sensor and heater locations are labeled in Figure 1.

Before final assembly, each of the low and medium force heads was validated by replacing the copper sample with a load cell, as shown in Figure 2. This load cell was used to quantify the amount of force exerted by the low and medium force heads as well as to ensure a repeatable assembly procedure.

Each fixture was validated based on approximate thermal interface material thicknesses. It was found that the low force heads applied a room temperature clamping force of 57.8 ± 4.4 N, which translated to 248.2 ± 20.7 kPa across an area of 2.32 mm^2 in this application. The medium force heads applied a room temperature clamping force of 427.0 ± 26.7 N, or 1838.8 ± 115.1 kPa. The results of the validation can be found in Figure 3. Note that the clamping force exerted by the fixture at 4 K is slightly higher than at

room temperature due to temperature dependent material properties. The clamping force applied by the fixture at 4 K could not be measured, so it was predicted using material properties from Ledbetter [5] and TPRC Data Series [6]. Further details can be found in the Discussion section. The low force heads applied a predicted clamping force of 62.3 ± 4.4 N at 4 K. The medium force heads applied a predicted clamping force of 456.4 ± 26.7 N at 4 K. Sample area was held constant.

Figure 2. Force test load cell installation.

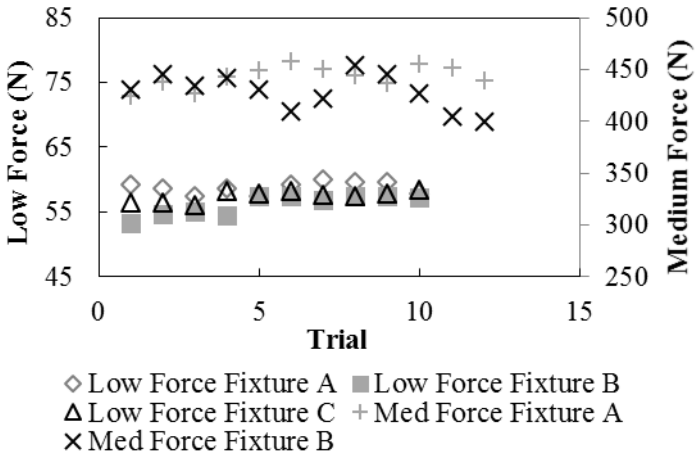

Figure 3. Low and medium force head validation at room temperature.

Each thermal interface material required specific preparation. All indium foil used for testing was 0.051 mm thick and was cut to match the footprint of the copper sample. Apiezon-N grease was applied directly to the copper sample and then spread as thinly as possible by hand with the intent of applying only enough grease to fill the surface roughness of the copper. The resulting thickness of grease was not measured. Gold plated samples and interposers were prepared per ASTM-B-488-01, TYPE III, CODE C, excluding the Ni layer, resulting in a 1.27-2.54 μm gold plate.

Where noted, the surface roughness of the copper was polished, taking it from a standard machine surface finish of 1.6 μm to a polished surface finish of 0.1 μm. **Table 1** details the specific setup of each test case.

Table 1. Test case matrix.

	Bulk Material	Thermal Interface Material	4 K Force (N)	Surface Roughness (μm)
1	OFHC Copper	Dry	62.3	1.6
2	OFHC Copper	Indium Foil	62.3	1.6
3	OFHC Copper	Apiezon-N	62.3	1.6
4	OFHC Copper	Dry	458.4	1.6
5	OFHC Copper	Indium Foil	458.4	1.6
6	OFHC Copper	Apiezon-N	458.4	1.6
7	OFHC Copper	Gold Plated	62.3	1.6
8	OFHC Copper	Gold Plated	62.3	0.1
9	OFHC Copper	Gold Plated	458.4	1.6

3. Test Procedure

Before installation, each test piece was cleaned with isopropyl alcohol. Copper samples 1-6 were also cleaned with a 400 grit Scotch-Brite® pad prior to being cleaned with isopropyl alcohol. This increased the surface roughness of the samples, but removed surface oxides. Indium foil was not cleaned.

Each test fixture was assembled with a validated low or medium force head. The thermal interface material of interest was applied as referenced above, and the sample was centered on the interposer. The springs inside the test fixture were then gradually released until the full compression force was applied. Once fully assembled, three test fixtures at a time were installed on the 4 K cryostat sample stage. The final assembly is shown in Figure 4. Lastly, the heater and temperature sensor wires were connected within the cryostat.

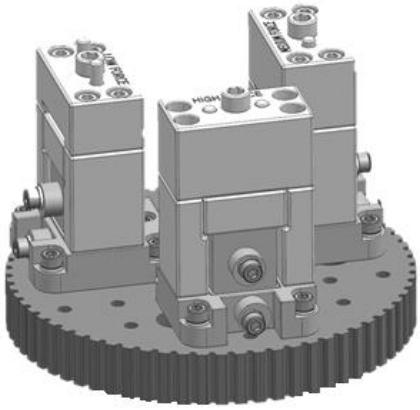

Figure 4. Final test configuration.

An RDK145 GM Cryocooler was used to test the samples in a 4 K radiation environment with 200 mW of heat lift capability. This environment was achieved by installing a 4 K radiation shield over the test assembly and attaching the shield to the 4 K sample stage. A 77 K radiation shield was then installed, followed by a 300 K radiation shield and vacuum jacket. The overall system was then pumped down to a 10^{-8} torr vacuum and a sample stage temperature of 2.8 K.

Once the system reached steady state, the samples were individually tested. For each sample, an initial power of approximately 0.01 W was applied to the Kapton heater. The current supplied to this heater was then gradually increased, and the voltage was recorded using a four wire measurement. At each power level the temperature of the interposer and the temperature of the copper sample were recorded.

As the temperature difference between the interposer and the copper sample increased with the increase in heater power, an additional heater was used to raise the base temperature of the cryostat sample stage. This base temperature adjustment was used in order to keep the temperature difference between the interposer and the copper sample to an average of 0.32 ± 0.01 K and no greater than 1.50 K ± 0.01 K. The power and base temperature were continually increased until temperature measurements across the thermal interface material were obtained between 3 K and 20 K.

4. Results

In order to create a baseline, a dry copper to copper interface was tested at both low and medium force. In this test both the sample and interposer had a standard surface finish of 1.6 μm before cleaning. The results of this testing, shown in Figure 5, closely followed a power law relationship as predicted by Salerno and Kittel for metallic pressed contacts [1]. Performance increased by a factor of approximately 4.4 from low to medium force. In all conductance figures the temperature plotted on the x-axis is the measured interposer temperature. The error bars represent the total measurement error associated with each sensor and instrument, as given by the uncertainty equation (4), where w is uncertainty, V is the measured voltage and I is the measured current.

$$wG=\sqrt{\left(\frac{\delta G}{\delta V}wV\right)^2+\left(\frac{\delta G}{\delta I}wI\right)^2+\left(\frac{\delta G}{\delta T_S}wT_S\right)^2+\left(\frac{\delta G}{\delta T_{Int}}wT_{Int}\right)^2} \quad (4)$$

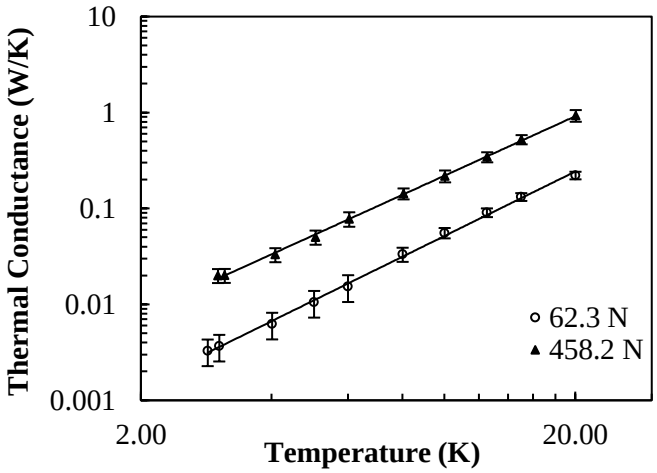

Figure 5. Dry copper to copper contact thermal conductance at low and medium clamping forces.

It was also shown that the contact thermal resistance of a 0.051 mm thick indium foil interface closely followed a power law relationship. Again, an increase of performance was seen with an increase of clamping force, as shown in Figure 6, and these results showed improved performance over those presented by Ekin [2], however the surface roughness and indium foil thickness presented in Ekin is unknown. The performance increased with force by a factor of approximately 3.4.

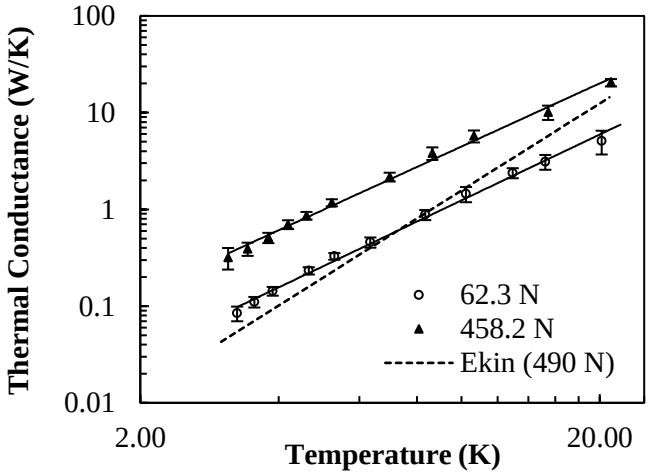

Figure 6. Indium foil contact thermal conductance at low and medium clamping forces.

While the performance of the Apiezon-N greased interface steadily increased from 2.8 K to 5 K, the performance plateaued at temperatures above 5 K. Figure 7 shows the difference in performance between low and medium clamping forces was found to be negligible.

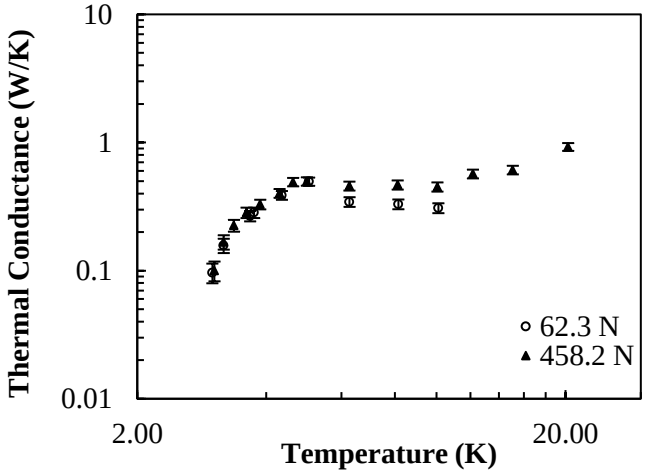

Figure 7. Apiezon-N grease contact thermal conductance at low and medium clamping forces.

Standard surface finish samples and interposers that were gold plated showed a steady increase in performance with the exception of a temperature region from 5 K to 10 K where increases in performance slowed. A polished surface finish sample was also gold plated, and the performance improved when compared to the standard surface finish sample at the same clamping force, as shown in Figure 8. The polished sample also showed a steadier increase in performance in the 5 K to 10 K temperature range.

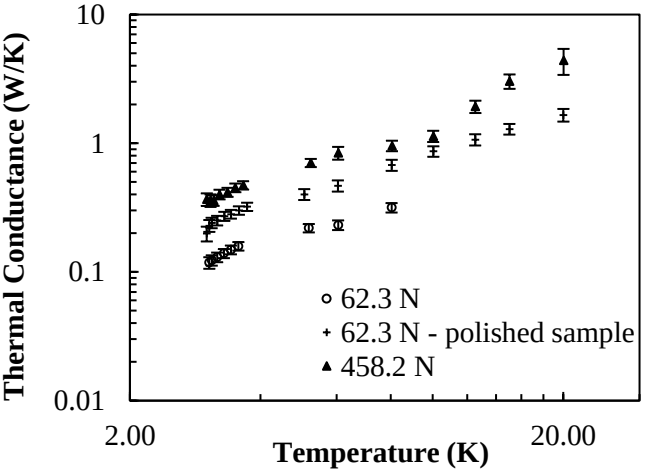

Figure 8. Gold plated copper contact thermal conductance at low and medium clamping forces.

Figure 9 shows the contact thermal conductance of each of the tested interfaces at a low clamping force of 62.3 N. At low temperatures the polished and gold plated sample demonstrated the highest conductance, while at temperatures above 6 K the indium foil interface achieved the highest conductance. The power law trend lines are again shown for the dry and indium foil interfaces.

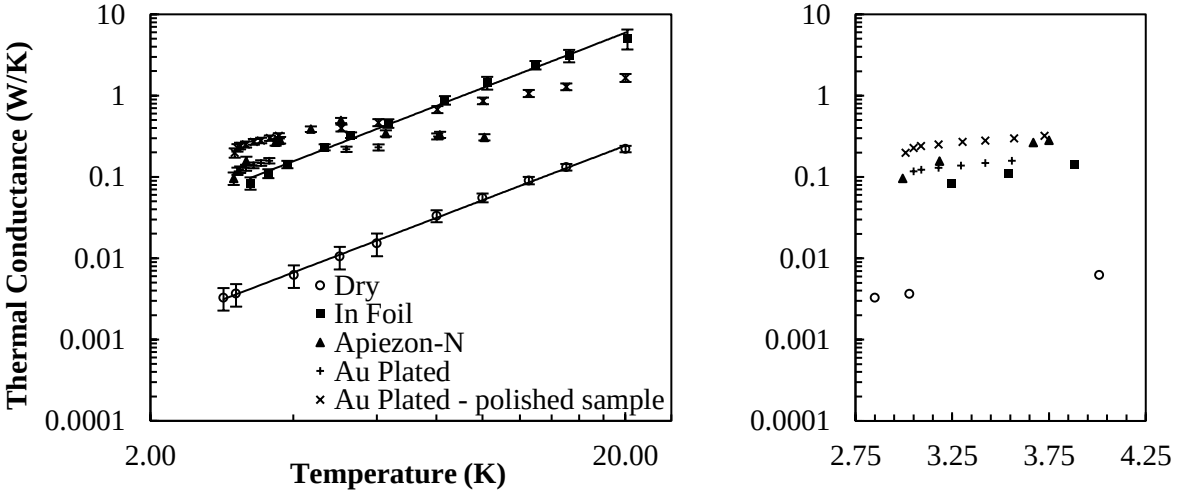

Figure 9. Comparison of contact thermal conductance for several thermal interface materials at 62.3 N of clamping force. Detailed view from 2.75 K to 4.25 K (right) less error bars and trend lines.

At a medium clamping force of 458.2 N the indium foil interface consistently showed the highest thermal performance across the full tested temperature range. A polished, gold plated sample was not tested at medium force. The compiled medium force results are presented in Figure 10, with power law trend lines shown for the dry and indium foil interfaces.

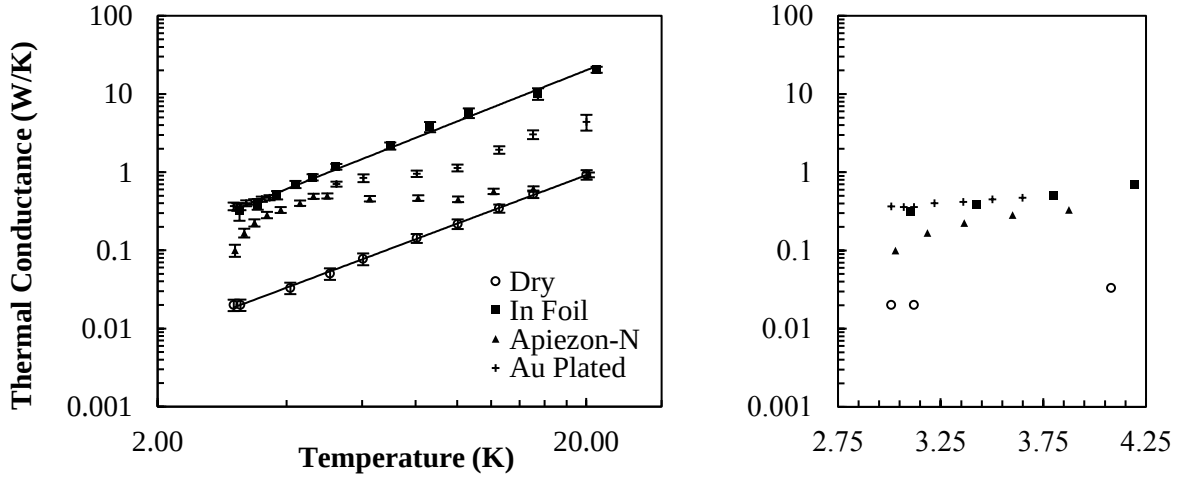

Figure 10. Comparison of contact thermal conductance for several thermal interface materials at 458.2 N of clamping force. Detailed view from 2.75 K to 4.25 K (right) less error bars and trend lines.

5. Discussion

The fixtures were fabricated primarily from 300 series stainless steel and OFHC copper. Stainless steel was chosen not only for its low thermal conductivity but also for its high strength and desirable CTE characteristics. The structural properties of stainless steel and OFHC copper are well known at cryogenic temperatures and thus predictable. The total material contraction of stainless steel and OFHC copper are quite similar from room temperature to 4 K. The difference in contraction was compensated in these fixtures by the use of Invar washers, springs, and appropriate fastener preloads.

As the fixture was cooled from room temperature to 4 K the forces applied by the springs were affected by the material characteristics of the fixture. The elastic modulus of the spring material increased by approximately 8% and therefore increased the force applied to the samples. Due to thermal contraction differences between the steel fixture and the copper sample, samples experienced a small decrease in force: a 0.022 N decrease for the low force head and a 4.89 N decrease for the medium force head. The combined effects of the increased elastic modulus of the spring material and the decreased compression from thermal contraction differences resulted in a net increase in compression force at 4 K compared to room temperature.

The material composition of the test setup was also selected in order to minimize the amount of heat leak through the non-critical heat path. The two pieces surrounding the thermal interface material, the sample and the interposer, were fabricated from OFHC copper to create a preferential heat path from the heater through the interface material. The pusher, springs, and other structural components of the fixture were fabricated from stainless steel to minimize the amount of heat traveling through these components rather than the interface material. The final test setup was modeled using ANSYS Icepak 17.2 in order to verify that the expected heat path calculations were valid. A depiction of the heat path is shown in Figure 11, and the amount of heat leak through the structural components of the fixture was approximately 7% when compared to the measured interface behavior. This heat leak value was subtracted out of the total power applied to the sample before computing the temperature rise through the copper and the interface.

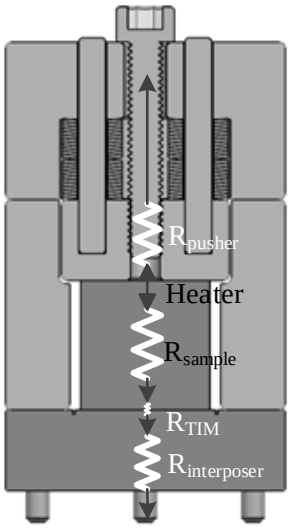

Figure 11. Cross section of thermal heat path through test fixture.

The change in temperature across the thermal interface, equation (1), was calculated by subtracting the temperature rise through the copper between the temperature sensors and the interface from the measured temperature difference. Utilizing equation (3), the temperature dependent thermal conductivity of copper with an RRR value of 125 was used to calculate the temperature rise through the copper [3]. This RRR value was determined from experimental conductivity measurements of copper received from the same vendor that manufactured the copper sample and interposer, and the associated error with this measurement was included in the TIM conductance error calculation. The resulting interface temperature difference was then used in equation (2) to calculate the thermal conductance across the interface.

Across all temperatures measured, the highest thermal conductance was achieved with an indium foil interface and a clamping force of 458.2 N. At low temperatures and the same clamping force, the thermal conductance of the gold plated interface was comparable to that of indium. At a clamping force of

62.3 N, the highest thermal conductance at low temperatures was achieved with a polished, gold plated copper sample and a standard surface finish, gold plated copper interposer. At temperatures above 6 K and 62.3 N of clamping force, the indium foil interface thermal conductance was consistently the highest. At all forces and temperatures the lowest thermal conductance was measured across the dry, standard surface finish copper to copper interface as expected. The main source of error in the conductance calculations was the applied power measurement, and the average measurement error in thermal conductance was approximately 12%.

6. Conclusion

With the behavior of several thermal interfaces characterized with this test setup and in agreement with several results previously presented in literature, the future work of this study will be to test the behavior of more complex packaging interfaces. Some interfaces of interest include further exploration into polished surfaces, applications of high force, and indium cold welding. The use of various bulk materials such as silicon will also be explored. Due to the demonstrated favorable performance of gold plating and indium foil, applications of polished, gold plated copper at high forces will be of particular interest as well as applications of indium cold welding. By testing desired packaging interfaces such as these we are able to directly measure thermal performance as it will be applied in a cryogenic electronic packaging application.

7. References

[1] Salerno L J and Kittel P 1997 Thermal contact conductance *NASA Technical Memorandum* 110429
[2] Ekin J W 2006 *Experimental Techniques for Low-Temperature Measurements Cryostat Design, Material Properties, and Superconductor Critical Current Testing* 2006 (Oxford University Press) chapter 2 pp 63
[3] Van Sciver S W 2012 *Helium Cryogenics* (New York: Springer) chapter 2 pp 35-44
[4] Kerr A R and Horner N 1991 The low temperature thermal resistance of high purity copper and bolted joints *Electronics Division Technical Note No. 163* (Charlottesville: National Radio Astronomy Observatory)
[5] Ledbetter H M 1982 Temperature behaviour of Young's moduli of forty engineering alloys (Butterworth & Co)
[6] Touloukian Y S, Kirby R K, Taylor R E and Desai P D 1975 Thermal expansion metallic elements and alloys *Thermophysical Properties of Matter – the TPRC Data Series* **12** (New York: IFI/Plenum Data Company)